

# Mitochondrial Creatine Kinase Binding to Phospholipids Decreases Fluidity of Membranes and Promotes New Lipid-Induced $\beta$ Structures As Monitored by Red Edge Excitation Shift, Laurdan Fluorescence, and FTIR<sup>†</sup>

Thierry Granjon,<sup>‡</sup> Marie-Jeanne Vacheron,<sup>‡</sup> Christian Vial,<sup>\*,‡</sup> and René Buchet<sup>§</sup>

Laboratoire de Biomembranes et Enzymes Associés and Laboratoire de Physico-Chimie Biologique, UMR 5013 "Reconnaissance et Transduction Moléculaires", Université Claude Bernard Lyon 1, 69622 Villeurbanne Cedex, France

Received October 2, 2000; Revised Manuscript Received February 28, 2001

**ABSTRACT:** Structural modifications induced by the binding of mitochondrial creatine kinase (mtCK) to saturated and unsaturated phospholipids were monitored by using Laurdan, a membrane probe sensitive to the polarity of the environment. The abrupt change characteristic of a phase transition of lipids alone was attenuated by addition of mtCK. Generalized polarization spectra indicated that mtCK surface binding changed the phospholipid liquid-crystalline state to a more rigid state. Infrared spectra of lipids further strengthened these results: upon mtCK binding, the phospholipid methylene chains had a more rigid conformation than that observed without mtCK at the same temperature. After mtCK binding to vesicles of perdeuterated dimyristoylphosphatidylcholine and nondeuterated dimyristoylphosphatidylglycerol, no lateral phase separation was observed, suggesting that both lipids were rigidified. Moreover, mtCK bound to liposomes exhibited an uncommon red edge excitation shift of 19 nm, while that of the soluble enzyme was only 6 nm. These results indicated that the environment of some mtCK tryptophan residues was motionally restricted. Strong stabilization of the enzyme structure against heat denaturation was observed upon lipid binding. In addition, lipids promoted a new reversible protein–protein or protein–lipid interaction, as evidenced by infrared data showing a slight modification of the  $\beta$  sheet over  $\alpha$  helix ratio with formation of a new 1632-cm<sup>-1</sup>  $\beta$  sheet instead of the soluble protein 1636-cm<sup>-1</sup> one. Such modifications, inducing a decrease in the fluidity of the mitochondrial membranes, may play a role in vesicle aggregation; they could be implicated in the appearance of contact sites between internal and external mitochondrial membranes.

CK<sup>1</sup> isoenzymes catalyze the reversible transfer of the phosphoryl group from phosphocreatine to ADP, regenerating ATP. These enzymes are expressed in tissues with important and rapid energy requirements. They are involved in a system referred to as the "phosphocreatine shuttle" (1–3). Three cytosolic isoenzymes, namely, MMCK (muscle), BBCK (brain), and MBCK (heart, lungs, stomach) (4, 5), and two mitochondrial (mtCK) isoforms, ubiquitous and sarcomeric (6, 7), have been identified. The cytosolic isoenzymes are exclusively in a dimeric form, whereas the mtCK are found in two active, interconvertible oligomeric states: a dimer and an octamer (8–10). MtCK is bound as an octamer to

the outer face of the inner membrane of mitochondria (8). Its level is especially high at the contact sites between the inner and the outer membranes (11, 12).

Although the mtCK binding site is not yet known, cardiolipin is thought to be part of this site, most likely through its negative charges (13). Indeed, the protein can also bind to vesicles containing acidic phospholipid, and this interaction appears to be largely of an ionic nature (14). As monitored by turbidity measurements, mtCK causes vesicle aggregation. This ability of mtCK to bridge the membranes, raising a network, could explain the propensity of protein to mediate contacts between membranes made from lipid extracts of the inner and outer mitochondrial membranes (15, 16) as well as to form crystals on a cardiolipin matrix (17). The X-ray structure of chicken mtCK provided further insight into the interaction of subunits and a better understanding of the octameric mtCK role in the mitochondrial membrane (18). The mtCK octamers display a cubelike structure with identical top and bottom faces that are thought to interact with the two mitochondrial membranes and to facilitate intermembrane contact site formation.

The characterization of mtCK in a lipid environment will enable us to understand the contribution of the membrane to the structure and function of the protein. In this work, for the first time, the fluorescence of Laurdan, red edge excitation

<sup>†</sup> This work was supported by grants from the Region Rhône-Alpes and the CNRS program "Physique et Chimie du Vivant".

<sup>\*</sup> To whom correspondence should be addressed at the Laboratoire de Biomembranes et Enzymes Associés, Université Claude Bernard Lyon 1, 43 boulevard du 11 novembre 1918, F-69622 Villeurbanne Cedex, France. Tel.: 33-(0) 4-72-44-82-48; Fax: 33-(0) 4-72-43-15-57; E-mail: christian.vial@univ-lyon1.fr.

<sup>‡</sup> Laboratoire de Biomembranes et Enzymes Associés.

<sup>§</sup> Laboratoire de Physico-Chimie Biologique.

<sup>1</sup> Abbreviations: CK, creatine kinase; mtCK, mitochondrial creatine kinase; CL, cardiolipin; DMPC, dimyristoylphosphatidylcholine; dDMPC, perdeuterated dimyristoylphosphatidylcholine; DMPG, dimyristoylphosphatidylglycerol; FTIR, Fourier transform infrared spectroscopy; GP, generalized polarization; PC, phosphatidylcholine; PE, phosphatidylethanolamine; PG, phosphatidylglycerol; REES, red edge excitation shift.

shift (REES), and infrared spectroscopy were associated to investigate mtCK binding to liposomes.

To monitor the physical state (gel or liquid-crystalline) of membranes after their interaction with mtCK, we used the spectral properties of an amphiphilic fluorescent probe, Laurdan (6-dodecanoyl-2-dimethylaminonaphthalene). This probe is sensitive to the polarity of the environment, displaying a large emission red shift in polar solvents due to a dipolar relaxation process (19, 20). It is thus extremely sensitive to the membrane state, and particularly to the molecular dynamics of the water molecules at the hydrophobic–hydrophilic boundary of the lipid bilayers (19, 21).

The generalized polarization concept (GP) was developed by Parasassi to quantify the membrane dynamics with fluorescence measurements. This parameter takes into account the variations of the fluorescence intensity of blue and red regions of emission or excitation spectra. Laurdan GP spectra enabled us to characterize the phospholipid physical state (19, 21, 22).

REES measurement, which is a novel approach to monitor the organization and the dynamics of a fluorophore environment under conditions of restricted mobility (23, 24), was used to characterize the environment of tryptophan residues of the soluble or liposome-bound mtCK. REES refers to the increase in the emission wavelength occurring when the excitation wavelength is shifted toward the red edge of the absorption band. Usually when a fluorophore is in a fluid medium the fluorescence emission wavelength is unchanged, irrespective of the excitation wavelength used. However, when the fluorophore is placed in a polar, viscous medium, its mobility is restricted. In such conditions, when the excitation wavelength is gradually shifted to longer wavelengths, a new population of fluorophores is excited and thus the fluorescence emission shifts to longer wavelengths (23, 25, 26). REES effects have only been observed with polar fluorophores in a polar solvent (23) and for proteins with a maximum emission wavelength between 325 and 340 nm, which is the case for mtCK and MMCK (24, 25).

Some information about the modifications caused by the binding of protein to liposomes was obtained by FTIR. This method allows us to monitor either protein secondary structure (27–31) or lipid structure (32). Infrared spectra of lipids were characterized by the  $\text{CH}_2$  (2850 and 2920  $\text{cm}^{-1}$ ) and  $\text{CH}_3$  (2870 and 2960  $\text{cm}^{-1}$ ) symmetrical and asymmetrical stretching vibrations, which are sensitive to the motional freedom of the methylene and methyl groups and thus to temperature, and to the membrane physical state (32–36). The ester  $\text{C}=\text{O}$  stretching band at about 1740  $\text{cm}^{-1}$  and the phosphate symmetric and asymmetric bands at around 1070 and 1200  $\text{cm}^{-1}$ , respectively, are sensitive to the formation of hydrogen bonds (37–40).

The aim of this work was to characterize the lipid–protein interactions to better understand the structure of the network promoted by mtCK with phospholipids, which can reflect the formation of the contact sites between mitochondrial membranes, and to specify the perturbations induced by protein binding to the structures of both the lipid bilayer and the mtCK.

## MATERIALS AND METHODS

**Materials.** MMCK was purchased from Boehringer Mannheim; mtCK was prepared and purified as previously

described (41). The purity of CK was established using high-resolution gel electrophoresis. Laurdan was purchased from Molecular Probes, and the phospholipids, bovine heart cardiolipin (CL), egg yolk phosphatidylcholine (PC), egg yolk phosphatidylethanolamine (PE), egg yolk phosphatidylglycerol (PG), dimyristoylphosphatidylcholine (DMPC), and dimyristoylphosphatidylglycerol (DMPG), were all obtained from Sigma. Perdeuterated dimyristoylphosphatidylcholine (dDMPC) was purchased from Avanti Polar Lipids. Phospholipid purity was checked by thin-layer chromatography. Deuterium oxide (99.9% isotopic purity) was purchased from Merck.

**Preparation of Liposomes.** Aliquots of the required lipids in chloroform solution were combined in the desired molar ratio, i.e.: PC–PE–CL (2:1:1), PC–PG (3:2), DMPC–DMPG (3:2), or dDMPC–DMPG (3:2). Lipids were kept above the gel to liquid-crystal transition temperature during liposome preparation. LUV were prepared by hydration and extrusion as previously described (14). Briefly, dry lipids were hydrated (20 mg/mL) in 20 mM Tris–HCl buffer, pH 7.4, and dispersed by vortexing to produce MLV. The lipid suspension was subjected to 6 freeze/thaw cycles and then extruded 19 times through a polycarbonate membrane (Nucleopore) with 0.4- and 0.2- $\mu\text{m}$  diameter pores using a mini-extruder. Extrusion through filters with 0.2- $\mu\text{m}$  pores yields homogeneous large unilamellar vesicles, with a mean diameter of about 0.14–0.15  $\mu\text{m}$  as determined by quasi-elastic light scattering using a Zetasizer 3000 (Malvern).

**Fluorescence Measurements.** Fluorescence measurements were performed with a Hitachi F4500 fluorometer (150-W Xe). The excitation and emission band-pass values were 2.5 and 5 nm, respectively. Spectra were recorded 20 min after addition of CK to the liposomes, using a 1-cm path length thermostated quartz cuvette. All fluorescence spectra were corrected for the baseline spectra of the buffer solution to remove the contribution of the Raman band.

Experiments with Laurdan were conducted as follows: phospholipids (DMPC–DMPG, 3:2) and Laurdan in chloroform solution were mixed in a 400:1 molar ratio, and the liposomes were then prepared as previously described. Laurdan excitation and emission spectra were recorded from 15 to 40 °C, using a 441-nm emission wavelength or a 361-nm excitation wavelength on either 60  $\mu\text{g}$  of Laurdan–liposomes (110  $\mu\text{M}$  DMPC–DMPG, 0.274  $\mu\text{M}$  Laurdan) or Laurdan–liposomes in the presence of 60  $\mu\text{g}$  of protein (0.2  $\mu\text{M}$  mtCK or 0.8  $\mu\text{M}$  MMCK), with or without 0.15 M NaCl. The final volume was adjusted to 800  $\mu\text{L}$  with 20 mM Tris–HCl buffer (pH 7.4). For experiments involving PC–PE–CL liposomes, Laurdan (1.4 mM in dimethyl sulfoxide) was added to the preformed liposomes at the same 400:1 molar ratio.

The excitation spectra of Laurdan present three kinds of modifications with increasing temperature due to phase transition of the phospholipids: (i) the two maxima observed shift from 361 and 380 nm at 15 °C to 355 and 375 nm at 40 °C, respectively; (ii) this shift is associated with a global fluorescence intensity decrease; (iii) a greater decrease in the 380-nm peak than in the 361-nm one is observed, leading to a modification of the  $\text{IF}_{361}/\text{IF}_{380}$  ratio where  $\text{IF}_{361}$  and  $\text{IF}_{380}$  are the fluorescence intensities at 361- and 380-nm excitation wavelength, respectively. When temperature increases, the maximum wavelength of the emission spectrum is shifted

from 441 nm at 15 °C to 490 nm at 40 °C. These observations are consistent with published data (19, 42, 43).

The excitation generalized polarization was calculated as

$$GP_{exc} = (I_g - I_l)/(I_g + I_l)$$

where  $I_g$  and  $I_l$  are the fluorescence intensities at the maximum emission wavelength in the gel (441 nm) and in the liquid-crystalline (480 nm) phases at a fixed excitation wavelength (361 nm). Emission GP is obtained in the same way, using the fluorescence intensity at the maximum excitation wavelength in the gel ( $I_g$ ) and in the liquid-crystalline ( $I_l$ ) phases at a fixed emission wavelength. Excitation and emission GP spectra were obtained by calculating excitation and emission GP values at each excitation or emission wavelength, respectively.

For REES measurements, the assays were carried out using mtCK or MMCK (18  $\mu$ g) in 800  $\mu$ L of 20 mM Tris-HCl buffer (pH 7.4), in the presence or absence of PC-PG or DMPC-DMPG liposomes (30  $\mu$ g of phospholipids). The maximum emission wavelength was measured at 5-nm excitation wavelength intervals from 275 to 310 nm.

**Infrared Spectra.** Liposomes (DMPC-DMPG, molar ratio 3:2, or PC-PE-CL, 2:1:1) were prepared as previously described, using 20 mM Tris-HCl- $^2$ H $_2$ O (pH 7.4) buffer. Perdeuterated DMPC-DMPG (3:2) liposomes were prepared in 20 mM Tris-HCl (H $_2$ O). The liposome suspension (240  $\mu$ g of phospholipids), or the lyophilized protein (300  $\mu$ g) dissolved in 20 mM Tris-HCl- $^2$ H $_2$ O buffer (30  $\mu$ L), pH 7.4, was incubated for 5 min at 30 °C in the FTIR cells prior to measurements. For assay with protein, the liposome suspension (240  $\mu$ g of phospholipids) was mixed with 300  $\mu$ g of enzyme in 20 mM Tris-HCl buffer, pH 7.4, and then incubated at 30 °C for 20 min. The removal of nonadsorbed protein and buffer was performed by centrifugation at 160000g for 20 min (Beckman Airfuge). The pellet was resuspended in 30  $\mu$ L of Tris- $^2$ H $_2$ O or Tris-H $_2$ O buffer for DMPC-DMPG or dDMPC-DMPG liposomes, respectively, so that the final CK concentration was 10 mg/mL.

The pH was measured with a glass electrode and was corrected by a value of 0.4 according to Glasoe and Long (44). Samples were loaded between two CaF $_2$  circular cells, with a 50- $\mu$ m Teflon spacer. FTIR spectra were recorded with a Nicolet 510 M FTIR spectrometer which was continuously purged with dry air. The infrared cell was thermostated with a water circulation bath. The nominal spectral resolution was 4 cm $^{-1}$ ; 256 scans were collected and co-added per sample spectrum, and Fourier-transformed for each sample. Every FTIR spectrum was representative of at least three independent measurements. The infrared spectra of buffer and residual water vapor were subtracted from the infrared spectrum of the sample.

## RESULTS

**Temperature Dependence of Laurdan Excitation GP in DMPC-DMPG Liposomes.** To visualize the possible modifications in the membrane structure which can be induced by mtCK interaction with the phospholipids (DMPC-DMPG, 3:2), we measured Laurdan GP variations. MMCK was used as a negative adsorption control. Figure 1 shows the excitation GP values as a function of temperature for Laurdan-liposomes alone or in the presence of mtCK or

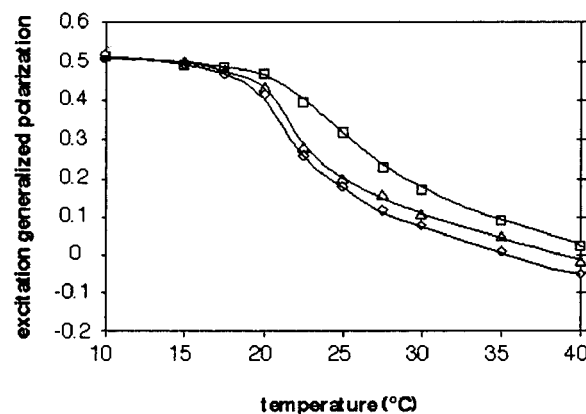


FIGURE 1: Excitation generalized polarization values as a function of temperature. 60  $\mu$ g of Laurdan-liposomes (DMPC-DMPG) alone (diamonds), with 60  $\mu$ g of mtCK (squares) or 60  $\mu$ g of MMCK (triangles). The GP<sub>exc</sub> values were obtained as described under Materials and Methods using a 361-nm excitation wavelength and emission intensities at 441 nm (gel-crystalline phase) and 480 nm (liquid-crystalline phase). The phospholipids to protein molar ratio was 500 with mtCK and 125 with MMCK. The Laurdan: phospholipid ratio was 1:400. Samples were suspended in a 800- $\mu$ L final volume of 20 mM Tris-HCl, pH 7.4.

Table 1: Measurements of Enzyme Binding and Liposome Aggregation

sample	binding (%) <sup>a</sup>	absorbance <sup>b</sup>
liposomes		0.008
mtCK + liposomes	78	0.400
mtCK + liposomes + NaCl, 0.15 M	0	0.130
MMCK + liposomes	3.4	0.012
MMCK + liposomes + NaCl, 0.15 M	3.6	0.015

<sup>a</sup> Binding assays were carried out with 150  $\mu$ g of phospholipids and 7  $\mu$ g of protein in 30  $\mu$ L of 20 mM Tris-HCl, pH 7.4, and the percentage of binding was determined from activity measurements in supernatants and pellets after centrifugation, as described by Vacheron et al. (14).

<sup>b</sup> The absorbance at 450 nm were measured with 60  $\mu$ g of phospholipids and 60  $\mu$ g of protein in 800  $\mu$ L of 20 mM Tris-HCl, pH 7.4.

cytosolic MMCK. Results with Laurdan-liposomes alone indicated that the excitation GP value was strongly affected by the temperature, showing a clear-cut change which demonstrated that the gel to liquid-crystalline phase transition occurred at around 22 °C. In the presence of mtCK, excitation GP values steadily decreased, indicating a progressive modification of the phospholipid mobility and organization of the environment polarity when temperature increased. The excitation GP value at 15 °C in the presence of mtCK was identical to that obtained with Laurdan-liposomes alone, whereas the value at 40 °C was higher. Thus, mtCK binding to liposomes seemed to broaden and to shift the phospholipid phase transition to higher temperatures.

In the presence of MMCK, excitation GP values also decreased as a function of temperature in a similar way to liposomes alone. They were shifted, above 25 °C, to slightly higher values than liposomes, but to a lesser degree than after mtCK binding. This result seems to indicate a small environmental modification of the probe in the presence of MMCK, which is surprising since this protein did not bind to liposomes under these conditions. Lack of fixation was verified by measuring the percentage of protein bound to liposomes (Table 1). Activity measurements showed that MMCK did not bind to phospholipids, and the low turbidity demonstrated that liposomes did not aggregate under these



conditions, in contrast to mtCK which was bound and induced phospholipid vesicle aggregation.

To explain these observations, spectra of Laurdan in the presence of mtCK or MMCK without phospholipids were recorded (not shown). The Laurdan spectrum was not modified by mtCK; thus, these molecules did not interact with each other. In the presence of MMCK, a fluorescence intensity increase and a maximum emission shift of Laurdan to a lower wavelength were observed, indicating that the probe was exposed to a more hydrophobic environment, probably due to its binding to MMCK. Thus, the slight shift of the excitation GP values observed in Figure 1 can be explained by free Laurdan binding to MMCK.

**Laurdan GP Spectra in DMPC–DMPG Liposomes.** GP fluorescence spectra obtained at 15 and 40 °C were analyzed to determine the phospholipid physical state homogeneity (Figure 2). In the absence of protein, at 15 °C, both excitation and emission GP spectra of Laurdan-loaded liposomes (DMPC–DMPG, 3:2) showed very small variations, and they appeared to be practically independent of the wavelength used, as was expected for a pure gel state. At 40 °C, the excitation GP profile showed a slight negative slope while the emission GP profile exhibited slightly increasing values when the wavelength increased. These results indicated that the phospholipids were in a pure liquid-crystalline state. Addition of MMCK did not induce any change, whatever the temperature used, which was foreseeable since this protein did not bind under these conditions.

By contrast, mtCK binding modified the spectral appearance at 40 °C: (i) the excitation GP values (Figure 2a) strongly increased above 400 nm; (ii) the GP values were higher in the presence of mtCK than in its absence (Figure 2b); (iii) the emission GP values (Figure 2c) decreased between 420 and 450 nm, leading to a negative slope, and then it recovered the same slightly increasing slope observed without protein. Both results demonstrated that mtCK attachment tended to rigidify the membrane, due to the coexistence of gel and liquid-crystalline states. Although markedly less important than at 40 °C, these tendencies were also evident at 25 °C, around the phospholipid phase transition temperature (not shown). These variations are strongly attenuated at 15 °C since the DMPC–DMPG mixture is already in a gel phase.

The same experiments were carried out at 40 °C in the presence of 0.15 M NaCl which prevented mtCK binding. The absence of binding was verified by activity measurements in supernatant and pellet after centrifugation (Table 1). Under these conditions, the GP spectra profiles in the presence of mtCK or MMCK were identical to those obtained without protein (data not shown). These results confirmed that the above-mentioned variations of Laurdan–liposome GPs in the presence of mtCK were actually due to protein binding.

**Laurdan GP Spectra in PC–PE–CL Liposomes.** The previous results obtained with saturated lipids allowed us to magnify the lipid modifications caused by mtCK binding, since the phase transition temperature of saturated lipids was higher than that of the unsaturated lipids. To better match the lipid environment of the inner mitochondrial membranes, similar experiments were performed with liposomes containing unsaturated phospholipids (PC–PE–CL, 2:1:1) (Figure 3). Negative slopes were clearly observed on the GP

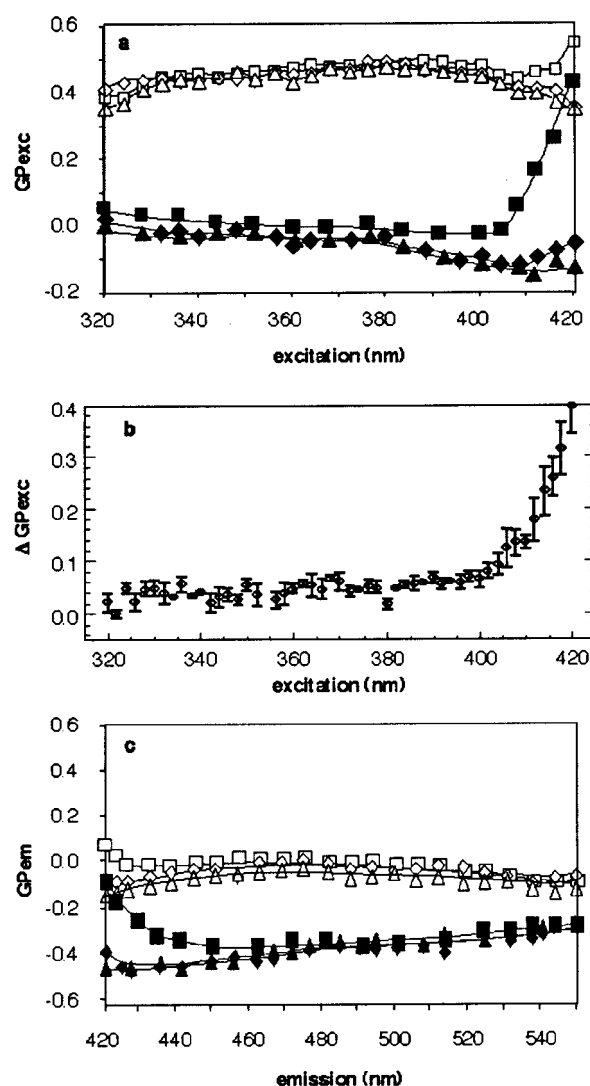


FIGURE 2: Laurdan excitation (a) or emission (c) generalized polarization spectra (see text) in 60  $\mu$ g of DMPC–DMPG vesicles alone (diamonds) or in the presence of 60  $\mu$ g of mtCK (squares) or MMCK (triangles) at 15 °C (open symbols) and 40 °C (filled symbols). (b) Variations of excitation GP as a function of excitation wavelength, where  $\Delta$ GP<sub>exc</sub> = excitation GP in the presence of mtCK minus excitation GP in the absence of mtCK (means of three experiments, error bars drawn from the minimal and maximal values). The phospholipids to protein molar ratio was 500 with mtCK and 125 with MMCK. The Laurdan:phospholipid ratio was 1:400. Samples were suspended in a 800- $\mu$ L final volume of 20 mM Tris-HCl, pH 7.4.

excitation spectra at both 15 and 40 °C, indicating that these phospholipids were in a liquid-crystalline state (Figure 3a). The binding of mtCK to liposomes induced a rise of the GP values, which was more important at 40 °C than at 15 °C and resulted from an increase in lipid chain order. However, this increase (about 0.12 at 420 nm) (Figure 3b) was less pronounced than that observed with liposomes made from saturated lipids (about 0.4) (Figure 2b). The comparison between the emission GP spectra of Laurdan in PC–PE–CL vesicles with and without mtCK (not shown) confirmed the coexistence of different lipid phases upon protein binding.

**REES of the Intrinsic Fluorescence.** The variation of the excitation wavelength slightly affected the MMCK maximum emission wavelength, indicating a small REES of 6 nm; soluble mtCK exhibited a similar pattern. The addition of PC–PG liposomes (Figure 4a) did not significantly modify

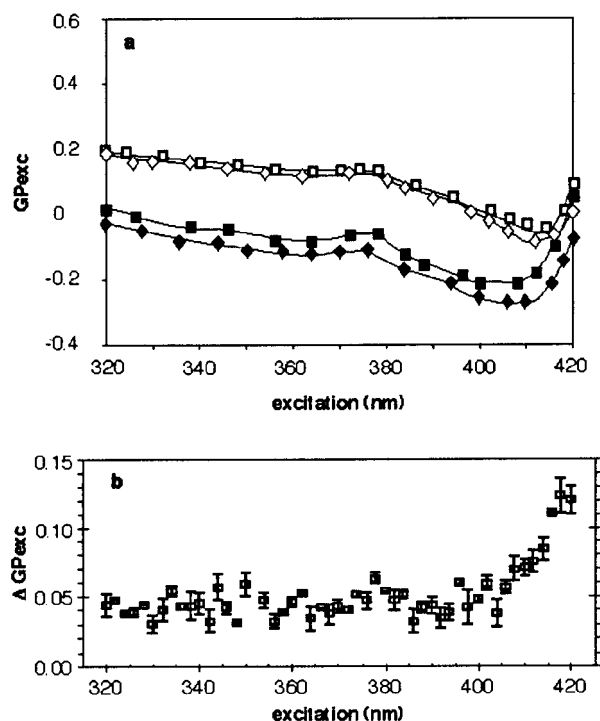


FIGURE 3: (a) Laurdan excitation generalized polarization spectra in 60 μg of PC-PE-CL vesicles alone (diamonds) or in the presence of 60 μg of mtCK (squares) at 15 °C (open symbols) and 40 °C (filled symbols). (b) Variations of excitation GP as a function of excitation wavelength, where  $\Delta GP_{exc}$  = excitation GP in the presence of mtCK minus excitation GP in the absence of mtCK (error bars drawn from the minimal and maximal values). The phospholipids to protein molar ratio was 500. The Laurdan: phospholipid ratio was 1:400. Samples were suspended in a 800-μL final volume of 20 mM Tris-HCl, pH 7.4.

the results obtained with MMCK alone, indicating that the tryptophan environment of MMCK was not modified by the presence of liposomes. In contrast, above an excitation wavelength of 295 nm, the binding of mtCK to unsaturated PC-PG (Figure 4a) as well as to saturated DMPC-DMPG

(Figure 4b) vesicles abruptly shifted the emission maximum to higher wavelengths, up to 350 nm. This corresponded to REES of 19 nm, implicating that the environment of some tryptophan residues in the bound mtCK was motionally restricted.

**Infrared Spectra of Lipid CH Groups.** To probe the effects of mtCK binding on the hydrocarbon chains of lipids, infrared spectra of liposomes containing saturated lipids (DMPC-DMPG) with and without protein were recorded. As a consequence of the shift of the CH<sub>2</sub> peak to higher wavenumbers, the intensity difference of the phospholipid asymmetric CH<sub>2</sub> stretching band at 2923 cm<sup>-1</sup> increased with temperature (Figure 5). The intensity of this band was not affected in the same way in the presence or in the absence of mtCK. Indeed, without protein the intensity change presented an inflection point at a transition temperature of around 25 °C. The presence of mtCK provoked a decrease in the intensity variations, with a shift of the inflection point toward a higher transition temperature.

Furthermore, at 30 °C, mtCK binding to liposomes induced a shift of symmetrical and asymmetrical CH<sub>2</sub> bands from 2854 to 2851 cm<sup>-1</sup> (Figure 6) and from 2923 to 2919 cm<sup>-1</sup>, respectively (not shown). At 30 °C, the 2854-cm<sup>-1</sup> and 2923-cm<sup>-1</sup> bands observed on the phospholipid spectrum, in the absence of protein, characterize the liquid-crystalline state of phospholipids, while those observed at 2851 and 2919 cm<sup>-1</sup> in the presence of mtCK at the same temperature reflect a higher degree of ordering of hydrocarbon chains.

After addition of 0.2 M NaCl to mtCK-coated liposomes, to promote solubilization of the protein, the spectrum in the symmetric CH<sub>2</sub> stretching area was identical to that of phospholipids alone (Figure 6). Thus, the effect observed on the phospholipid CH<sub>2</sub> vibrations should be due to the binding of mtCK to the liposomes, which makes the acyl chains less mobile.

Despite the very low variation in the intensity of the CH<sub>3</sub> stretching vibrations, there was a reproducible, albeit small, shift of the symmetrical CH<sub>3</sub> band toward a higher wave-

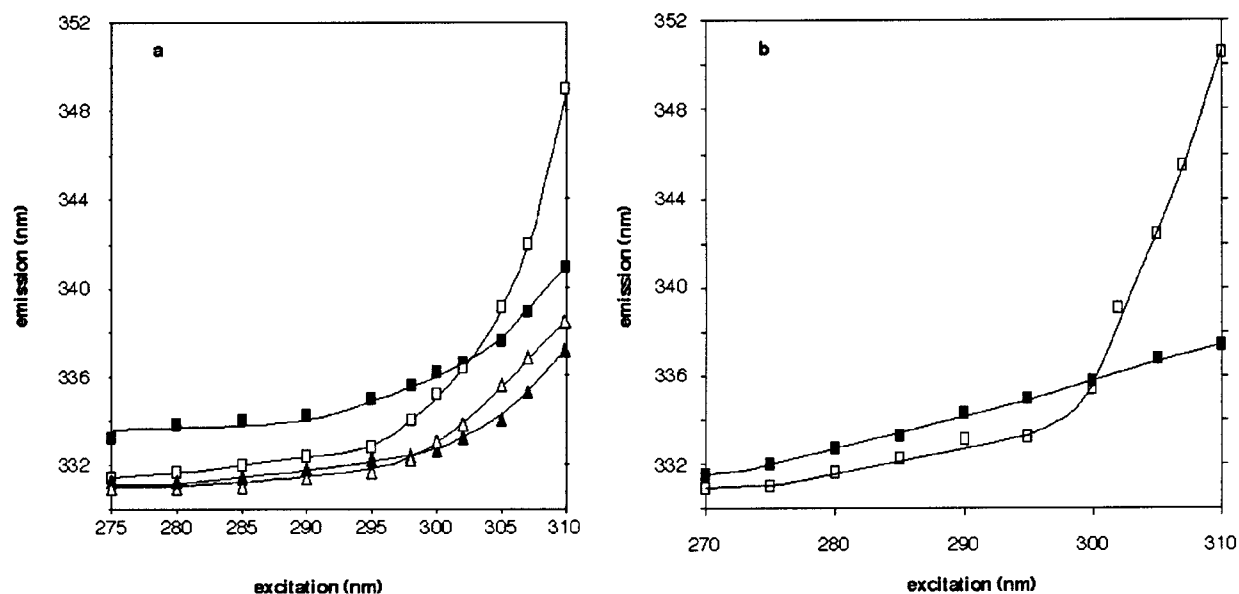


FIGURE 4: Red edge excitation shift. Maximum wavelength of the emission spectra at different excitation wavelengths of 18 μg of mtCK (squares) or MMCK (triangles), in the presence (open symbols) or absence (filled symbols) of (a) 30 μg of PC-PG liposomes or (b) 30 μg of DMPC-DMPG liposomes. Each point was the average of at least three determinations. The phospholipids to protein molar ratio was 832 for mtCK and 207 for MMCK. Samples were suspended in a 800-μL final volume of 20 mM Tris-HCl, pH 7.4.

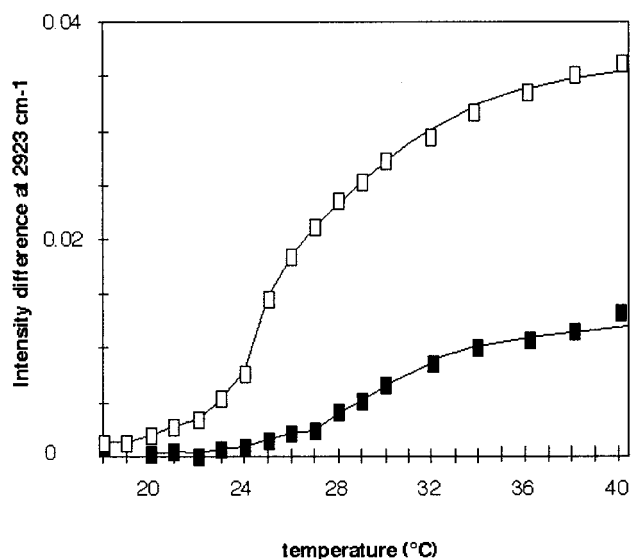


FIGURE 5: Intensity difference of the asymmetric  $\text{CH}_2$  stretching vibration, as a function of temperature, of  $240 \mu\text{g}$  of DMPC-DMPG liposomes alone (open symbols) or with  $300 \mu\text{g}$  of mtCK (filled symbols). Each point results from the difference between the absorbance measured at  $17^\circ\text{C}$  and the absorbance measured at the indicated temperature. Samples were prepared as described under Materials and Methods; the final volume was  $30 \mu\text{L}$  of  $20 \text{ mM}$  Tris-HCl- $^2\text{H}_2\text{O}$ ,  $\text{p}^2\text{H}$  7.4.

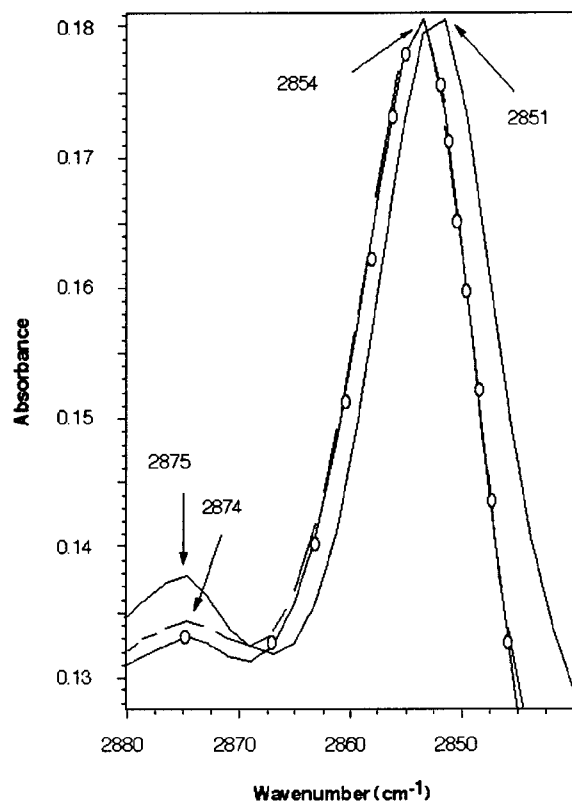


FIGURE 6: Infrared spectra, in the region of the symmetric  $\text{CH}$  stretching vibration, of  $240 \mu\text{g}$  of DMPC-DMPG liposomes alone (---), with  $300 \mu\text{g}$  of mtCK in the absence (—) or in the presence (O—O) of  $0.2 \text{ M}$  NaCl. Samples were suspended in  $30 \mu\text{L}$  of  $20 \text{ mM}$  Tris-HCl- $^2\text{H}_2\text{O}$ ,  $\text{p}^2\text{H}$  7.4, as described under Materials and Methods.

number upon mtCK binding from  $2874$  to  $2875 \text{ cm}^{-1}$ , suggesting a greater motional freedom of the  $\text{CH}_3$  groups of lipids in contrast to  $\text{CH}_2$  groups (Figure 6).

Vesicles containing unsaturated PC-PE-CL were used to monitor lipid-protein interactions under conditions approaching more closely the lipid composition of the biological membrane. At  $30^\circ\text{C}$ , upon mtCK binding, shifts of symmetrical and asymmetrical  $\text{CH}_2$  bands, from  $2855$  to  $2853 \text{ cm}^{-1}$  and from  $2925$  to  $2923 \text{ cm}^{-1}$ , respectively, were observed, indicating a population of ordered unsaturated lipids (not shown).

To check whether lateral phase separation occurred during mtCK binding to liposomes, perdeuterated DMPC in the DMPC-DMPG mixture was used. Addition of mtCK to liposomes produced shifts of symmetrical and asymmetrical  $\text{C}^2\text{H}_2$  bands of perdeuterated DMPC toward lower wavenumbers from  $2095$  to  $2091 \text{ cm}^{-1}$  and from  $2198$  to  $2195 \text{ cm}^{-1}$ , indicating that the protein induced a rigidification of DMPC phospholipids (Figure 7a). As showed in Figure 7b, similar shifts of  $\text{CH}_2$  bands to lower wavenumber were observed in the  $2800$ – $3000\text{-cm}^{-1}$  range, indicating that the binding of mtCK to the dDMPC-DMPG mixture also provoked an increase of rigidification of DMPG phospholipids.

**Infrared Spectra of Ester and Phosphate Groups of Phospholipids.** Alterations in hydrogen bonding, orientation of the headgroup, and differences in chain packing of phospholipids can be monitored at the  $\text{C}=\text{O}$  and  $\text{O}-\text{P}-\text{O}$  stretching vibration level ( $37$ – $40$ ). The DMPC-DMPG  $\text{C}=\text{O}$  vibrations at  $1740 \text{ cm}^{-1}$  did not significantly change in the presence or in the absence of mtCK (not shown), indicating that the protein binding did not cause any modification at the phospholipid carbonyl level and that there was no formation or breaking of the hydrogen bonds involving these carbonyl groups. However, the adsorption of mtCK to liposomes containing either saturated (Figure 8) or unsaturated (not shown) phospholipids resulted in a NaCl-sensitive shift of the symmetric  $\text{PO}_2^-$  stretching band from  $1089$  to  $1083 \text{ cm}^{-1}$  that can be interpreted as alterations in headgroup hydration or increased hydrogen bonding at the polar surface of phospholipids following protein fixation (39).

**Amide I Band.** The spectra of protein alone and bound to DMPC-DMPG liposomes in the amide I region are presented in Figure 9. The  $1651\text{-cm}^{-1}$  band corresponds to an  $\alpha$  helical structure, while the  $1630$ – $1636\text{-cm}^{-1}$  band is related to  $\beta$  sheets. When the protein was adsorbed, small variations of the  $\alpha/\beta$  ratio were observed, with a broadening of the band that may result from a shift of the  $\beta$  sheet band to lower wavenumbers at around  $1632 \text{ cm}^{-1}$ . Small changes were also observed when unsaturated phospholipids were used (not shown). To ascertain whether this new  $\beta$  sheet structure corresponded to denatured-aggregated  $\beta$  sheets, we performed temperature-induced denaturation under the same conditions. Figure 10, panel A, shows the difference spectra of the soluble protein as a function of temperature in the amide I region. Temperature increase induced the appearance of a peak at  $1616 \text{ cm}^{-1}$ , usually associated with an intermolecular  $\beta$  sheet structure, typical of aggregate formation observed during protein denaturation (45, 46). This appearance was related to a decrease in the  $\alpha$  helix content ( $1651 \text{ cm}^{-1}$ ) and  $\beta$  sheet structure ( $1636 \text{ cm}^{-1}$ ). When mtCK was bound to saturated lipids, Figure 10, panel B, clearly indicates the presence of a band which did not increase with temperature, centered at  $1632 \text{ cm}^{-1}$  instead of  $1636 \text{ cm}^{-1}$  for the soluble enzyme. The temperature-dependence varia-

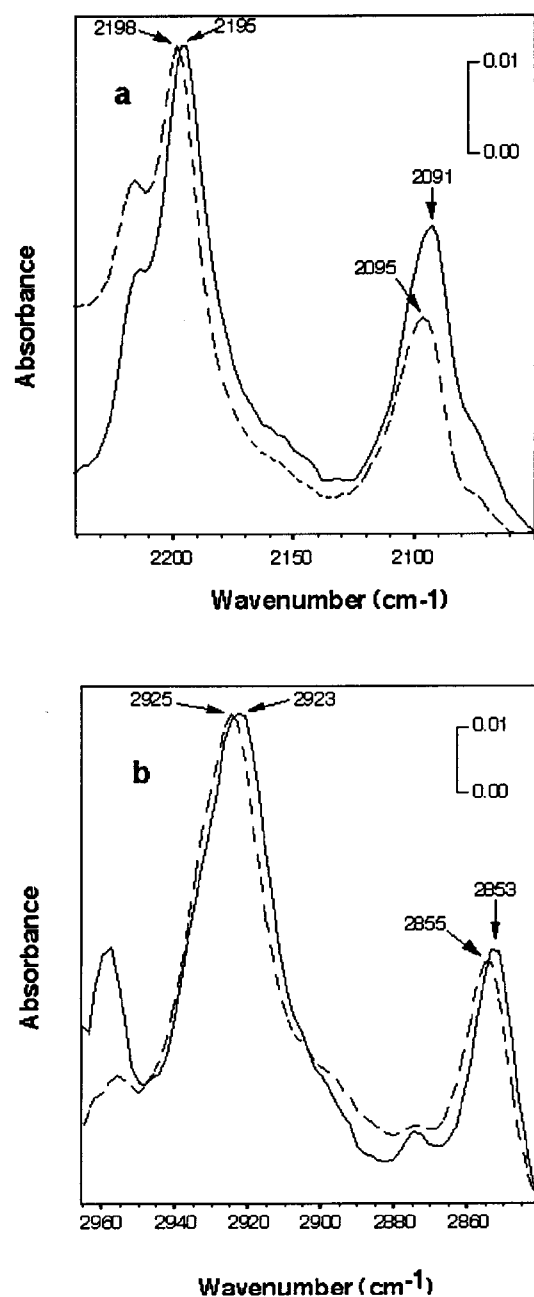


FIGURE 7: Infrared spectra, in the region of C<sup>2</sup>H (a) and CH (b) stretching vibrations, of 240  $\mu$ g of dMPC–DMPG liposomes alone (---) or with 300  $\mu$ g of mtCK (—). Samples were suspended in 30  $\mu$ L of 20 mM Tris-HCl, pH 7.4, as described under Materials and Methods.

tions of 1616, 1636, and 1651  $\text{cm}^{-1}$  were strongly attenuated when mtCK was bound to DMPC–DMPG liposomes [Figure 10, panel C, trace (c)] as compared with mtCK alone [Figure 10, panel C, trace (a)], showing that the association with lipids stabilized the enzyme structure against thermal denaturation and suggesting that the 1632- $\text{cm}^{-1}$  band cannot be assigned to protein denaturation.

In addition, association of mtCK with unsaturated PC–PE–CL lipids led to an almost identical stabilization against heat denaturation, although it was slightly smaller than with saturated lipids, as indicated by the 1616- $\text{cm}^{-1}$   $\beta$ -denaturation band [Figure 10, panel C, trace (b)]. Therefore, secondary structure changes of mtCK induced by its binding to unsaturated or saturated lipids were quite similar.

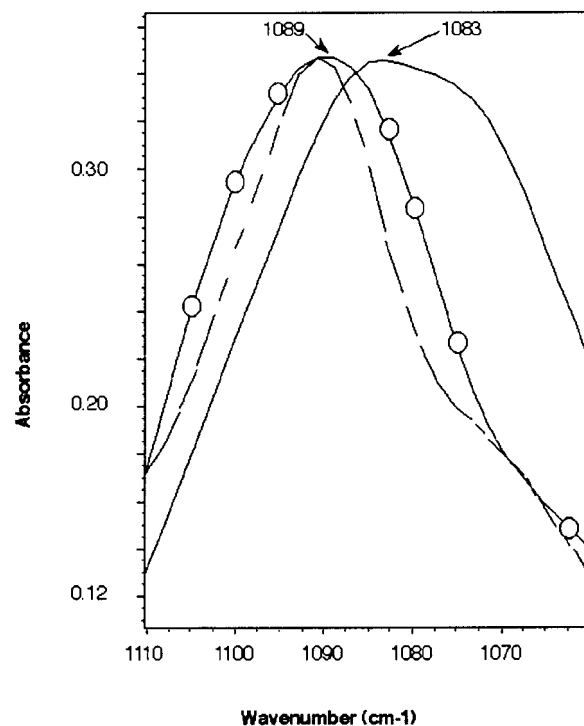


FIGURE 8: Infrared spectra, in the region of the symmetric  $\text{PO}_2^-$  stretching vibration, of 240  $\mu$ g of DMPC–DMPG liposomes alone (---), with 300  $\mu$ g of mtCK in the absence (—) or in the presence (O–O) of 0.2 M NaCl. Samples were suspended in 30  $\mu$ L of 20 mM Tris-HCl– $^2\text{H}_2\text{O}$ , pH 7.4, as described under Materials and Methods.

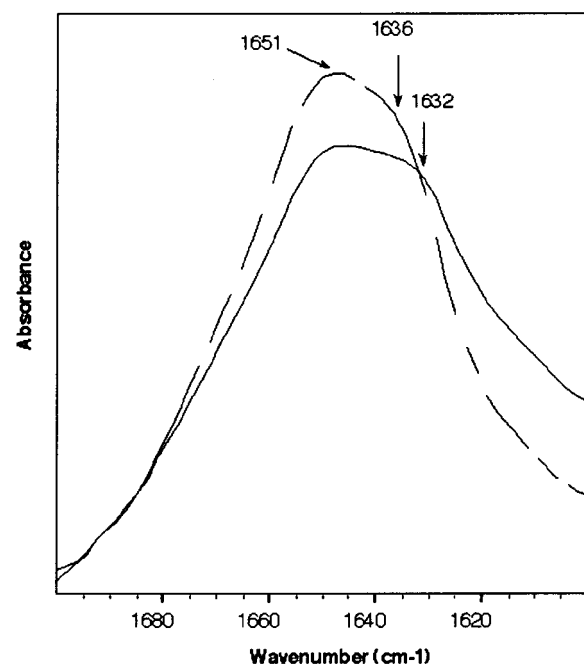


FIGURE 9: Infrared spectra, in the region of the amide I band, of 300  $\mu$ g of soluble mtCK (---) and 300  $\mu$ g of mtCK bound to 240  $\mu$ g of DMPC–DMPG liposomes (—) at 30  $^{\circ}\text{C}$ . Samples were suspended in 30  $\mu$ L of 20 mM Tris-HCl– $^2\text{H}_2\text{O}$ , pH 7.4, as described under Materials and Methods.

## DISCUSSION

*Fluorescence of Laurdan Inserted in Liposomes Containing Saturated or Unsaturated Lipids.* The extreme sensitivity of the fluorescence membrane probe Laurdan to the polarity of the environment as well as to the surrounding water



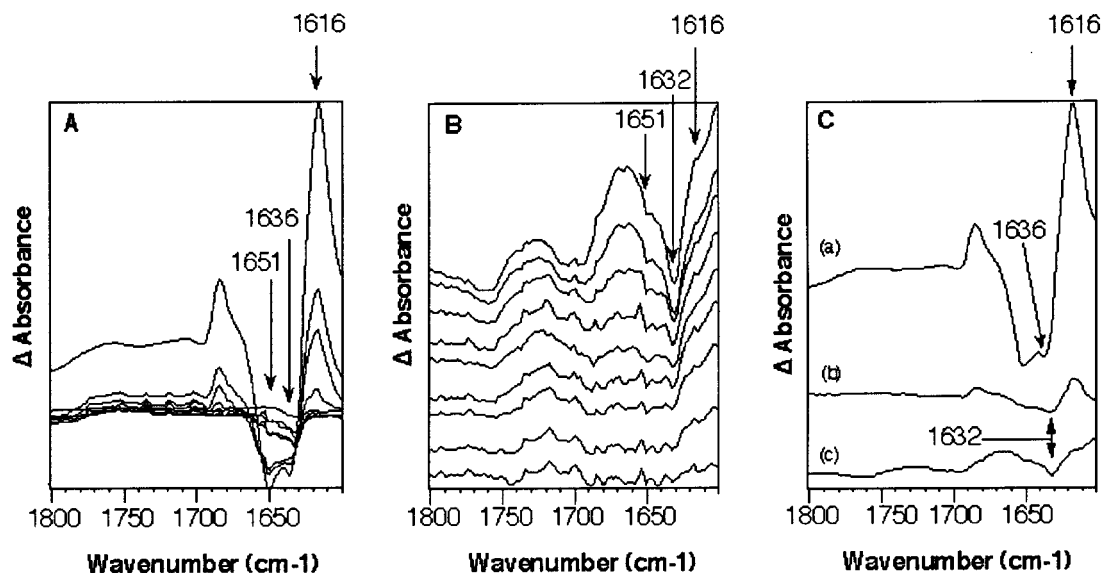


FIGURE 10: Difference infrared spectra, in the region of the amide I band, of 300  $\mu\text{g}$  of soluble mtCK (panel A) or 300  $\mu\text{g}$  of mtCK bound to 240  $\mu\text{g}$  of DMPC-DMPG liposomes (panel B). Each difference spectrum corresponds to the difference of spectra measured at two temperatures: 35 – 30 °C; 40 – 30 °C; 45 – 30 °C; 50 – 30 °C; 55 – 30 °C; 60 – 30 °C; 65 – 30 °C; 70 – 30 °C; and 75 – 30 °C from the bottom to the top. Panel C: Difference infrared spectra of 300  $\mu\text{g}$  of soluble mtCK (a) and 300  $\mu\text{g}$  of mtCK bound to either 240  $\mu\text{g}$  of PC-PE-CL liposomes (b) or 240  $\mu\text{g}$  of DMPC-DMPG liposomes (c) at 75 – 30 °C with the same scale. Samples were suspended in 30  $\mu\text{L}$  of 20 mM Tris-HCl- $^2\text{H}_2\text{O}$ , p $^2\text{H}$  7.4, as described under Materials and Methods.

dynamics makes it a good tool to characterize the physical state of the phospholipids in which Laurdan is inserted and to monitor the consequences of the mtCK adsorption. With increasing temperature, mtCK binding to DMPC-DMPG liposomes produces greater excitation GP values than in the absence of protein (Figure 1). This can be interpreted as a decrease in the interactions between Laurdan and the adjacent water molecules. Furthermore, the abrupt excitation GP variation, that is characteristic of the phospholipid phase transition, is attenuated after mtCK adsorption. This broadening of the phospholipid phase transition temperature was often observed with natural or reconstituted membrane preparations containing proteins (47–49). However, in our case the binding of mtCK to liposomes increased the phase transition temperature, suggesting a rigidification of the membrane rather than an increase of the phospholipid disorder, which generally follows the interaction of integral proteins with the lipid membrane (50–52). Adsorption of mtCK seems to have an effect on the Laurdan environment similar to that of the reduction in polarity induced by cholesterol addition to a phospholipid bilayer (42).

The GP spectra of Laurdan in DMPC-DMPG liposomes with or without mtCK or MMCK provide new insights about the environment modification observed after mtCK interaction. At 40 °C, in the absence of protein, the decrease in the excitation GP values (Figure 2a) associated with the increase in the emission GP values (Figure 2c), with increasing wavelength, indicated a dipolar relaxation process of solvent molecules, without any specific selection of Laurdan molecules in different physical states (49). These results characterized Laurdan molecules inserted into phospholipids in a pure liquid-crystalline state. At 15 °C, GP spectra did not show any wavelength dependence, demonstrating the insertion of Laurdan in a pure phospholipid gel phase.

At 40 °C, mtCK causes a strong increase in the excitation GP spectrum slope above 400 nm, and a decrease in the emission GP spectrum slope between 420 and 450 nm

(Figure 2a,c). This suggests that Laurdan is inserted in a mixed gel and liquid-crystalline phospholipid state. The binding of the protein to the phospholipid membrane would decrease either the surrounding water mobility, as already shown by the excitation GP increase observed as a function of temperature (Figure 1), or the number of water molecules. At 15 °C, GP spectra exhibit no prominent modification upon addition of the proteins to the liposomes. At this temperature, saturated phospholipids are already in a pure gel phase and the modification of the probe environment after mtCK binding is much smaller than at 40 °C.

Thus, the binding of mtCK to liposomes modified the phospholipid fluidity and changed the liquid-crystalline state to a more rigid state, eventually leading to a mixture of lipid states, which could explain the broadening of the phase transition observed in Figure 1.

To approach the actual composition of the inner mitochondrial membrane, liposomes were prepared with a mixture of unsaturated PC-PE-CL lipids. Although at the used temperatures unsaturated lipids are in a more disordered liquid-crystalline state than saturated lipids, GP values were higher after protein binding (Figure 3). However, this effect was of smaller magnitude than that observed with saturated lipids. In both cases, at 40 °C in the presence of protein, excitation GP values in the 420-nm region were quite similar to those obtained at 15 °C (Figures 2a and 3a). This indicated that mtCK binding produced an increase of a population of ordered lipids which tends to decrease the fluidity of the membrane.

*Intrinsic Fluorescence of MtCK Bound to Saturated or Unsaturated Lipids.* The red shift exhibited by the maximum emission wavelength (REES) arises from the slow rate of solvent relaxation around an excited-state fluorophore. It enables us to monitor the environment-induced motional restriction that is imposed on solvent molecules in the fluorophore vicinity (24, 25). Both MMCK and mtCK show a small REES of 6 nm (Figure 4), indicating that tryptophan



motion in these proteins is not totally free. The presence of liposomes did not modify the MMCK tryptophan environment. However, when mtCK is bound to liposomes with saturated or unsaturated lipids, the 19-nm REES suggests that the dipolar moment relaxation lifetime of the solvent is lower than the tryptophan fluorescence lifetime of mtCK. This large REES, which compares with the highest values of literature data (53–55), indicated that tryptophan residues are localized in a region that offers an important resistance to the solvent dipolar moment reorientation. This motionally restricted environment could correspond to a location in a region that is near the protein–membrane interface, where charge interactions and hydrogen bonding are involved (26, 55). However, this possibility is unlikely since, according to the three-dimensional structure, the tryptophan residues are located in the inner core of the protein (18). Alternatively, this REES could result from a structural modification of the protein due to mtCK binding to liposomes. This conformational change would decrease the mobility of the environment of some tryptophan residues.

*Effect of MtCK on the Infrared Spectra of Liposomes Containing Saturated or Unsaturated Lipids.* The increase in the phospholipid acyl chain flexibility as a function of temperature was evidenced by the variation of the intensity difference at  $2923\text{ cm}^{-1}$  (asymmetric  $\text{CH}_2$  stretching band). As expected for DMPC–DMPG liposomes, a phase transition temperature of about  $25^\circ\text{C}$  was observed (Figure 5). The binding of mtCK to DMPC–DMPG liposomes induced a shift in the phospholipid transition phase to a higher temperature and also induced a decrease in the variation of the intensity of the  $\text{CH}_2$  vibrations, indicating a more rigid phospholipid state.

At  $30^\circ\text{C}$ , the symmetric  $\text{CH}_2$  vibration of saturated phospholipids is located at  $2854\text{ cm}^{-1}$  (Figure 6), corresponding to phospholipids mainly in a liquid-crystalline state (32). The binding of mtCK shifted both the asymmetric and symmetric  $\text{CH}_2$  bands of lipids to lower wavenumbers. Upon mtCK binding, the phospholipid methylene chains changed to a more rigid conformation compared with phospholipids alone at the same temperature. This structural modification is due to protein binding, since mtCK desorption by NaCl enabled phospholipids to recover a structure similar to that observed in the absence of protein.

The variations in the  $\text{CH}_3$  band at  $2874\text{ cm}^{-1}$  must be carefully analyzed because of its lower intensity with regard to that of the  $\text{CH}_2$  band. However, the  $\text{CH}_3$  band shifted to a higher wavenumber in the opposite direction to that observed for the  $\text{CH}_2$  band. This change reflects a greater motional freedom of the acyl chain extremities as seen after cholesterol insertion (35). As already reported, in a gel phase (DMPC), the  $\text{CH}_3$  mobility is higher than that of  $\text{CH}_2$ , probably due to the decrease in the interdigitation of the hydrocarbon chains (36).

The results obtained with these lipid models are clear-cut. However, their biological relevance could be challenged. Therefore, liposomes containing unsaturated PC–PE–CL lipids were prepared. Despite their higher hydrocarbon disordering as compared with saturated lipids, addition of mtCK also promoted a rigidification of the chains as evidenced by the unambiguous  $\text{CH}_2$  vibrational modes. Comparison between saturated and unsaturated lipids allowed

us to strengthen some aspects of lipid–protein interaction and to anticipate those that were not easily observed.

To assess whether mtCK binding to liposomes promoted a lateral phase separation of phospholipids, DMPC–DMPG liposomes were prepared with perdeuterated DMPC. Both  $\text{C}^2\text{H}_2$  (perdeuterated DMPC, Figure 7a) and  $\text{CH}_2$  (DMPG, Figure 7b) regions of the infrared spectra showed a shift to lower wavenumber upon mtCK binding, suggesting an increase of the ordered hydrocarbon chain population of both lipids, without lateral phase separation. It is tempting to propose that upon mtCK interaction promoting lipid aggregation, propagated lipid–lipid or lipid–protein interactions restricted the mobility of the head polar groups, causing a rigidification of the hydrocarbon chains of lipids.

The lipid  $\text{C}=\text{O}$  band position, assessing the degree of hydrogen bonding, was not affected after protein adsorption, indicating that the hydration layer at the phospholipid hydrophobic–hydrophilic interface was not modified (37). On the other hand, significant changes were apparent in the region of phosphate stretching vibrations (Figure 8): they shifted to a lower wavenumber following mtCK adsorption to liposomes containing either saturated or unsaturated lipids. This result suggested that the phosphate moieties become involved in stronger hydrogen bonding interactions and/or in electrostatic interactions with charged groups of the protein (56, 57). Protein binding to phospholipids would lead to stronger interactions between mtCK and phosphate headgroups than those between phosphate groups and water, inducing an immobilization of polar heads which is consistent with the membrane fluidity decrease previously observed.

*Amide I Band.* A close analysis of the amide I region revealed small differences between free and bound mtCK in the  $1630\text{--}1660\text{ cm}^{-1}$  region (Figure 9). The protein difference spectra (Figure 10, panel A) showed that increasing temperature induced the aggregation of the free protein, characterized by the band centered at about  $1616\text{ cm}^{-1}$ . The intensity increase of this band is associated with a concomitant decrease in the  $\alpha$  helix and  $\beta$  sheet structures, as indicated by the decrease in the intensities at  $1651$  and  $1636\text{ cm}^{-1}$ . However, as shown in Figure 10 panel C, the protein structure was strongly heat-stabilized upon binding to saturated and unsaturated phospholipids since the observed variations in intensities were significantly smaller than those obtained with free mtCK. In addition, this experiment indicated the presence of a new  $\beta$  sheet structure after binding to liposomes evidenced by a band centered at  $1632\text{ cm}^{-1}$ . This band is not related to the aggregation of heat-denatured protein since it tends to disappear upon heating of the bound enzyme. It could correspond to protein–protein interactions induced by binding to phospholipids, such as those which have been observed on negatively charged lipid layers (17). Alternatively, the protein binding to liposomes could induce a shift in the  $\beta$  sheet band from  $1636$  to  $1632\text{ cm}^{-1}$  (Figure 9), arising from an increase in hydrogen bonding caused by the lipid hydrophobic environment, as has been observed with other proteins (46, 58). This latter structural modification was better evidenced with saturated lipids.

## CONCLUSION

Analysis of both fluorescence and FTIR results led to the same conclusion: the electrostatic binding of mtCK to

DMPC—DMPG liposomes induced the broadening of the phospholipid phase transition temperature and a decrease in phospholipid mobility. This result is consistent with those observed in the case of annexin V, a protein which can form electrostatic interactions with anionic phospholipids making the vesicle bilayers more rigid (59). This is in contrast to membrane proteins which usually increase lipid disorder (50–52). Until now, no structural modifications of mtCK upon binding to a membrane structure have been reported. REES data indicated a modification of the protein tryptophan surroundings upon binding to liposomes composed of either saturated or unsaturated lipids, suggesting that of one or several tryptophan residues interacted with a motionally restricted environment. This restricted mobility resulting from the mtCK—membrane interaction would arise either from the tryptophan location near the protein—membrane interface or, more probably, from a structural change of the protein. In addition, FTIR analysis revealed new protein—protein or protein—phospholipid interactions upon mtCK binding. Protein—protein interactions could be favored by the high concentration of mtCK used for FTIR experiments and could be related to its known ability to form ordered aggregates. The binding to phospholipids would be necessary to promote such protein—protein interactions. This phenomenon could be related to the formation of intramitochondrial inclusion bodies observed in muscle mitochondria of patients suffering mitochondrial disorders or in cells grown in a creatine-depleted medium (60).

Furthermore, the ability of mtCK to raise a network and bridge the membranes could explain the propensity of protein to mediate contact sites between internal and external mitochondrial membranes (15). These contact points, allowing for the passage of energetic substrates through the membranes, would make both phospholipid and mtCK less mobile. Since mtCK affected both types of lipids in DMPC—DMPG liposomes, it is tempting to suggest that the enzyme modified the ordering not only of the first range of lipids surrounding the protein (mostly negatively charged) but also of the neighboring molecules (including neutral lipids).

The fluidity alteration of the membrane induced by mtCK could influence the mitochondrial function as suggested in the case of annexin V binding, especially at the level of cardiolipin-dependent enzymes, such as respiratory complexes or carrier proteins (59, 61–63). As far as our results with DMPC—DMPG and PC—PE—CL liposomes can be extended to biological membranes, the decrease in fluidity may have some significance in the functional coupling between oxidative phosphorylation, adenine nucleotide translocase, porin, and mtCK (64, 65). The rigidification of phospholipid microdomains of the mitochondrial membrane could perturb the enzymes inserted in these membranes, affecting their functions. Furthermore, the change in fluidity could contribute to explain the role of mtCK in the formation and function of the mitochondrial permeability pores which are involved in the apoptosis process (66, 67). Taken together, these results open new perspectives on the physiological role of mtCK in the cells.

## ACKNOWLEDGMENT

We thank Dr. Cyrille Raimbault for preliminary experiments and helpful discussion.

## REFERENCES

1. Saks, V. A., Rosenshtraukh, L. V., Smirnov, V. N., and Chazov, E. I. (1978) *Can. J. Physiol. Pharmacol.* 56, 691–706.
2. Bessman, S. P., and Geiger, P. J. (1981) *Science* 211, 448–452.
3. Wallimann, T., and Eppenberger, H. M. (1985) in *Cell and Muscle Motility* (Shay, I. W., Ed.) pp 239–285, Plenum Publishing Corp., New York.
4. Dawson, D. M., Eppenberger, H. M., and Kaplan, N. O. (1965) *Biochem. Biophys. Res. Commun.* 21, 346–349.
5. Eppenberger, H. M., Dawson, D. M., and Kaplan, N. O. (1967) *J. Biol. Chem.* 242, 204–209.
6. Jacobs, H. K., Heldt, H. W., and Klingenberg, M. (1964) *Biochem. Biophys. Res. Commun.* 16, 516–521.
7. Haas, R. C., and Strauss, A. W. (1990) *J. Biol. Chem.* 265, 6921–6927.
8. Marcillat, O., Goldschmidt, D., Eichenberger, D., and Vial, C. (1987) *Biochim. Biophys. Acta* 890, 233–241.
9. Schlegel, J., Zurbriggen, B., Wegmann, G., Wyss, M., Eppenberger, H. M., and Wallimann, T. (1988) *J. Biol. Chem.* 263, 16942–16953.
10. Schnyder, T., Gross, H., Winkler, H., Eppenberger, H. M., and Wallimann, T. (1991) *J. Cell Biol.* 112, 95–101.
11. Biermans, W., Bakker, A., and Jacobs, W. (1990) *Biochim. Biophys. Acta* 1018, 225–228.
12. Kottke, M., Adams, V., Wallimann, T., Nalam, V. K., and Brdiczka, D. (1991) *Biochim. Biophys. Acta* 1061, 215–225.
13. Müller, M., Moser, R., Chenaval, D., and Carafoli, E. (1985) *J. Biol. Chem.* 260, 3839–3843.
14. Vacheron, M. J., Clottes, E., Chautard, C., and Vial, C. (1997) *Arch. Biochem. Biophys.* 344, 316–324.
15. Rojo, M., Hovius, R., Demel, R. A., Nicolay, K., and Wallimann, T. (1991) *J. Biol. Chem.* 266, 20290–20295.
16. Rojo, M., Hovius, R., Demel, R., Wallimann, T., Eppenberger, H. M., and Nicolay, K. (1991) *FEBS Lett.* 281, 123–129.
17. Schnyder, T., Cyrklaff, M., Fuchs, K., and Wallimann, T. (1994) *J. Struct. Biol.* 112, 136–147.
18. Fritz-Wolf, K., Schnyder, T., Wallimann, T., and Kabsh, W. (1996) *Nature* 381, 341–345.
19. Parasassi, T., De Stasio, G., Ravagnan, G., Rusch, R. M., and Gratton, E. (1991) *Biophys. J.* 60, 179–189.
20. Bagatolli, L. A., Maggio, B., Aguilar, F., Sotomayor, C. P., and Fidelio, G. D. (1997) *Biochim. Biophys. Acta* 1325, 80–90.
21. Parasassi, T., De Stasio, G., d'Ubaldo, A., and Gratton, E. (1990) *Biophys. J.* 57, 1179–1186.
22. Bagatolli, L. A., Gratton, E., and Fidelio, G. D. (1998) *Biophys. J.* 75, 331–341.
23. Lakowicz, J. R., and Keating-Nakamoto, S. (1984) *Biochemistry* 23, 3013–3021.
24. Demchenko, A. P. (1988) *Trends Biochem. Sci.* 13, 374–377.
25. Mukherjee, S., and Chattopadhyay, A. (1995) *J. Fluoresc.* 5, 237–246.
26. Chattopadhyay, A., and Rukmini, R. (1993) *FEBS Lett.* 335, 341–344.
27. Byler, D. M., and Susi, H. (1986) *Biopolymers* 25, 469–487.
28. Surewicz, W. K., and Mantsch, H. H. (1988) *Biochim. Biophys. Acta* 952, 115–130.
29. Bandekar, J. (1992) *Biochim. Biophys. Acta* 112, 123–143.
30. Surewicz, W. K., Mantsch, H. H., and Chapman, D. (1993) *Biochemistry* 32, 389–394.
31. Goormaghtigh, E., Cabiaux, V., and Ruyschaert, J. M. (1994) in *Subcellular Biochemistry* (Hilderson, H. J., and Ralston, G. B., Eds.) pp 330–362 Plenum Press, New York.
32. Cameron, D. G., Casal, H. L., and Mantsch, H. H. (1980) *Biochemistry* 19, 3665–3672.
33. Casal, H. L., and Mantsch, H. H. (1984) *Biochim. Biophys. Acta* 779, 381–401.
34. Ben-Efraim, I., Kliger, Y., Hermesh, C., and Shai, Y. (1999) *J. Mol. Biol.* 285, 609–625.
35. Umemura, J., Cameron, D. G., and Mantsch, H. H. (1980) *Biochim. Biophys. Acta* 602, 32–44.

36. Severcan, F., Kazanci, N., Baykal, U., and Süzer, S. (1995) *Biosci. Rep.* 15, 221–229.
37. Wong, P. T. T., and Mantsch, H. H. (1988) *Chem. Phys. Lipids* 46, 213–224.
38. Wong, P. T. T. (1994) *Biophys. J.* 66, 1505–1514.
39. Lewis, R. N., Pohle, W., and McElhaney, R. N. (1996) *Biophys. J.* 70, 2736–2746.
40. Mantsch, H. H., and McElhaney, R. N. (1991) *Chem. Phys. Lipids* 57, 213–226.
41. Marcillat, O., Perraut, C., Granjon, T., Vial, C., and Vacheron, M. J. (1999) *Protein Expression Purif.* 17, 163–168.
42. Parasassi, T., Di Stefano, M., Loiero, M., Ravagnan, G., and Gratton, E. (1994) *Biophys. J.* 66, 120–132.
43. Hellgren, L. I. (1996) *Plant Physiol. Biochem.* 34, 455–463.
44. Glasoe, P. K., and Long, F. A. (1960) *J. Phys. Chem.* 64, 188–190.
45. Raimbault, C., Couthon, F., Vial, C., and Buchet, R. (1995) *Eur. J. Biochem.* 234, 570–578.
46. Garcia-Garcia, J., Corbalan-Garcia, S., and Gomez-Fernandez, J. C. (1999) *Biochemistry* 38, 9667–9675.
47. Palleshi, S., and Silvestroni, L. (1996) *Biochim. Biophys. Acta* 1279, 197–202.
48. Antollini, S. S., Soto, M. A., Bonini de Romanelli, I., Gutierrez-Merino, C., Sotomayor, P., and Barrantes, F. J. (1996) *Biophys. J.* 70, 1275–1284.
49. Parasassi, T., Loiero, M., Raimondi, M., Ravagnan, G., and Gratton, E. (1993) *Biochim. Biophys. Acta* 1153, 143–154.
50. Mendelsohn, R., and Mantsch, H. H. (1986) in *Progress in Protein-Lipid Interactions* (Watts, A., and De Pont, J. J. H. H. M., Eds.) pp 103–145, Elsevier, Amsterdam.
51. Vincent, J. S., and Lewin, I. W. (1988) *Biochemistry* 27, 3438–3446.
52. Gericke, A., Smith, E. R., Moore, D. J., Mendelsohn, R., and Storch, J. (1997) *Biochemistry* 36, 8311–8317.
53. Patra, S. K., and Pal, M. K. (1997) *Spectrochim. Acta, Part A* 53, 1609–1614.
54. Rawat, S. S., Mukherjee, S., and Chattopadhyay, A. (1997) *J. Phys. Chem. B* 101, 1922–1929.
55. Santos, N. C., Prieto, M., and Castanho, M. A. (1998) *Biochemistry* 37, 8674–8682.
56. Choma, C. T., and Wong, P. T. T. (1992) *Chem. Phys. Lipids* 61, 131–137.
57. Shibata, A., Ikawa, K., and Terada, H. (1995) *Biophys. J.* 69, 470–477.
58. Lewis, R. N. A. H., Prenner, E. J., Kondejewski, L. H., Flach, C. R., Mendelsohn, R., Hodges, R. S., and McElhaney, R. N. (1999) *Biochemistry* 38, 15193–15203.
59. Megli, M., Mattiazzi, M., Tullio, T., and Quagliariello, E. (2000) *Biochemistry* 39, 5534–5542.
60. O’Gorman, E., Piendl, T., Müller, M., Brdiczka, D., and Wallimann, T. (1997) *Mol. Cell. Biochem.* 174, 283–289.
61. Hoffmann, B., Stöckl, A., Schlame, M., Beyer, K., and Klingenberg, M. (1994) *J. Biol. Chem.* 269, 1940–1944.
62. Paradies, G., Petrosillo, G., and Ruggiero, F. M. (1997) *Biochim. Biophys. Acta* 1319, 5–8.
63. Kisselev, P., Tuckey, R. C., Woods, S. T., Triantopoulos, T., and Schwarz, D. (1999) *Eur. J. Biochem.* 260, 768–773.
64. Wyss, M., Smeitink, J., Wevers, R. A., and Wallimann, T. (1992) *Biochim. Biophys. Acta* 1102, 119–166.
65. Brdiczka, D., Kaldis, P., and Wallimann, T. (1994) *J. Biol. Chem.* 269, 27640–27644.
66. Beutner, G., Rück, A., Riede, B., Welte, W., and Brdiczka, D. (1996) *FEBS Lett.* 396, 189–195.
67. O’Gorman, E., Beutner, G., Dolder, M., Koretsky, A. P., Brdiczka, D., and Wallimann, T. (1997) *FEBS Lett.* 414, 253–257.

BI002293E